HHS Public Access

Author manuscript

Neurobiol Aging. Author manuscript; available in PMC 2016 March 01.

Published in final edited form as:

Neurobiol Aging. 2015 March ; 36(3): 1439–1450. doi:10.1016/j.neurobiolaging.2014.12.029.

PGE_2 receptor agonist misoprostol protects brain against intracerebral hemorrhage in mice

He Wu[a,b], **Tao Wu**[b,c], **Wei Hua**[a], **Xianghui Dong**[a], **Yufeng Gao**[b], **Xiaochun Zhao**[b], **Wenwu Chen**[b], **Wangsen Cao**[d], **Qingwu Yang**[e], **Jiping Qi**[a,*], **Jin Zhou**[f,*], and **Jian Wang**[b,*]

[a]Department of Pathology, First Clinical Hospital, Harbin Medical University, Harbin, China

[b]Department of Anesthesiology and Critical Care Medicine, Johns Hopkins University, School of Medicine, Baltimore, Maryland, USA

[c]Stroke Center, Stroke Screening and Intervention Base, Changhai Hospital, Second Military Medical University, Shanghai, China

[d]Department of Basic Medical Science, Nanjing University School of Medicine, Nanning, China

[e]Department of Neurology, Xinqiao Hospital, Third Military Medical University, Chongqing, China

[f]Department of Hematology, First Clinical Hospital, Harbin Medical University, Harbin, China

Abstract

Intracerebral hemorrhage (ICH) is a devastating form of stroke. Misoprostol, a synthetic PGE_1 analog and PGE_2 receptor agonist, has shown protection against cerebral ischemia. In this study, we tested the efficacy of misoprostol in 12-month-old mice subjected to one of two complementary ICH models, the collagenase model (primary study) and blood model (secondary study, performed in an independent laboratory). We also investigated its potential mechanism of action. Misoprostol post-treatment decreased brain lesion volume, edema, and brain atrophy and improved long-term functional outcomes. In the collagenase-induced ICH model, misoprostol decreased cellular inflammatory response; attenuated oxidative brain damage and gelatinolytic activity; and decreased HMGB1 expression, Src kinase activity, and interleukin-1β expression without affecting cyclooxygenase-2 expression. Further, HMGB1 inhibition with glycyrrhizin decreased Src kinase activity, gelatinolytic activity, neuronal death, and brain lesion volume. Src kinase inhibition with PP2 decreased gelatinolytic activity and brain edema and improved neurologic function, but did not decrease HMGB1 protein level. These results indicate that

*Corresponding authors: Jiping Qi, MD, PhD: Department of Pathology, First Clinical Hospital, Harbin Medical University, 23 Youzheng Road, Harbin 150001, China (Phone: 86.0451.85555809; Fax: 86.0451.85555045; qijiping2003@163.com), Jin Zhou, MD, PhD: Department of Hematology, First Clinical Hospital, Harbin Medical University, 23 Youzheng Road, Harbin 150001, China (Phone: 86.0451.53642767; Fax: 86.0451.53641824; zhoujin1960@hotmail.com), Jian Wang, MD, PhD: Department of Anesthesiology and Critical Care Medicine, The Johns Hopkins University, School of Medicine, 720 Rutland Ave, Ross Bldg 370B, Baltimore, MD 21205 (Phone: 443.287.5490; Fax: 410.502.5177; jwang79@jhmi.edu).

Disclosure statement

None of the authors has any actual or potential conflicts to declare.

misoprostol protects brain against ICH injury through mechanisms that may involve the HMGB1, Src kinase, and MMP-2/9 pathway.

Keywords

High-mobility group box 1; Inflammation; Matrix metalloproteinase; PGE_2; Src

1. Introduction

Intracerebral hemorrhage (ICH) is a devastating form of stroke that often leads to death or disability. The inflammatory cascade contributes to the progression of ICH-induced secondary brain injury (Wang, 2010; Wu, et al., 2010). Prostaglandin E_2 (PGE_2), which is predominant in the brain, is a lipid mediator that modulates neuroinflammation, including matrix metalloproteinases (MMPs) (Wang and Dore, 2007). Interestingly, macrophages in human atherosclerotic plaques secrete MMP-2 or MMP-9 through a PGE_2-dependent mechanism (Cipollone, et al., 2001). PGE_2 can bind four receptor subtypes (EP1–4) that each have a distinct signaling cascade. EP2 and EP4 receptors have protective effects in cerebral ischemia (Liang, et al., 2011; Liu, et al., 2005; McCullough, et al., 2004). Misoprostol, a synthetic PGE_1 analog and PGE_2 receptor EP2–4 agonist (Li, et al., 2008), is widely prescribed to patients for prophylaxis of nonsteroidal anti-inflammatory drug-induced ulcer disease because it restores the cytoprotective function of PGE_2 necessary for maintaining integrity of the gastric mucosa (Numo, 1992). Interestingly, recent studies have shown that misoprostol protects brain against cerebral ischemia via the PGE_2 EP2 and/or EP4 receptors (Li, et al., 2008; Taniguchi, et al., 2011). PGE_2 is reported to be produced and to accumulate in the perihematomal region in an ICH model (Chu, et al., 2004). However, whether misoprostol reduces brain injury after ICH remains unknown.

Patients with ICH have been reported to have high serum levels of high-mobility group box 1 (HMGB1) (Zhou, et al., 2010). Released from necrotic cells, HMGB1 is a cytokine that triggers inflammation and upregulates MMP-9 expression (Qiu, et al., 2010). MMP-9 is also regulated by Src kinases, a family of non-receptor protein tyrosine kinases that phosphorylate and regulate a number of molecules (Liu and Sharp, 2011). Importantly, inhibition of HMGB1 expression or Src kinase activity reduces early brain injury after ICH (Ardizzone, et al., 2007; Ohnishi, et al., 2011), and MMP-9 could be a potential downstream target (Liu and Sharp, 2011; Qiu, et al., 2010). Consistent with these findings, we and others have shown that inhibition of MMP-2/9 activity reduces brain injury after ICH (Wang and Tsirka, 2005a; Xue, et al., 2009b).

Although aging alters the efficacy and side effect profiles of many medications (Fisher, et al., 2009; Hurn, et al., 2005), most preclinical studies of ICH have been carried out in young animals. This practice limits the translation of preclinical studies into clinical trials. To avoid this pitfall and enhance the clinical relevance, we used 12-month-old mice in the current set of experiments. In the primary study, we subjected mice to the collagenase-induced ICH model and examined the hypothesis that misoprostol reduces early brain injury after ICH through mechanisms that involve the HMGB1/Src/MMP-2/9–mediated signaling pathway.

In the secondary study, we subjected mice to the whole blood ICH model and repeated experiments on drug efficacy in a separate laboratory to assess reproducibility in lesion volume, brain edema, and neurologic outcomes.

2. Materials and Methods

2.1. Animals

All animal experiments were approved by an institutional animal welfare committee and were performed in accordance with the National Institutes of Health guidelines. In two separate studies, we used 216 12-month-old C57BL/6 male mice (Charles River Laboratories, Wilmington, MA, USA; the center for Experimental Animals, Harbin Medical University, Harbin, China) because cerebrovascular effects of aging are well developed in mice at this age (Park, et al., 2007). The primary study was carried out in the Department of Anesthesiology and Critical Care Medicine, Johns Hopkins University School of Medicine, Baltimore, MD, and the secondary study was carried out in the Department of Pathology, First Clinical Hospital, Harbin Medical University, Harbin, China.

2.2. ICH models

In the primary study, we injected mice in the left striatum with collagenase VII-S (0.075 U in 500 nL saline, Sigma, St. Louis, MO) at the following stereotactic coordinates: 0.8 mm anterior and 2.0 mm lateral of the bregma, 2.9 mm in depth, as described previously (Grossetete and Rosenberg, 2008; Wang, et al., 2003). In the secondary study, 8 μL of autologous whole blood removed from the tail without anticoagulant was infused at a rate of 0.4 μL/minute into the left striatum, according to our published protocol (Wang, et al., 2008). Rectal temperature was maintained at 37.0 ± 0.5°C throughout the experimental and recovery periods. These two procedures resulted in reproducible lesions that were mostly restricted to the striatum. Sham groups had needle insertion only. Body weight was measured before and after collagenase or blood injection. Percent change in body weight was calculated as previously described (H. Wu, et al., 2011).

2.3. Experimental groups

Computer-generated random numbers were used for study group randomization. To assess the efficacy of misoprostol, we treated mice with subcutaneous injections of either vehicle (hydroxypropyl-methyl cellulose, HPMC) or misoprostol in HPMC (1 mg/kg; 1:100 misoprostol: HPMC; Pfizer, Groton, CT) at 2, 6, and 12 hours after ICH. The dosing regimen was based on published work that used rodent cerebral ischemia/hypoxia models (Li, et al., 2008; Taniguchi, et al., 2011). To inhibit HMGB1, we treated mice intraperitoneally (i.p.) with glycyrrhizin (100 mg/kg, pH = 7.0–7.5, Sigma-Aldrich, St. Louis, MO) or vehicle (saline) 2 hours post-ICH, and then once daily afterward for 3 days. To inhibit Src kinase activity, we treated mice i.p. with Src kinase inhibitor PP2 (4-amino-5-(4 chlorophenyl)-7-(t-butyl) pyrazolo [3,4-D] pyrimidine; 2.0 mg/kg, Cayman Chemical, Ann Arbor, MI) or vehicle (saline) at 2 hours after ICH. The dosing regimens of glycyrrhizin and PP2 were based on previous studies in rats (Liu, et al., 2008; Ohnishi, et al., 2011). The permeability of brain to misoprostol, glycyrrhizin, and PP2 has not been tested in mice. However, the blood-brain barrier opening after ICH would facilitate drug entry into

the brain. Investigators blinded to the treatment groups evaluated outcomes in all mice and performed calculations and analysis.

2.4. Neurologic deficit

We assessed neurologic deficit score in the misoprostol-treated and vehicle-treated groups on days 3 and 28 after ICH. Mice were evaluated on six neurologic subtests, including body symmetry, gait, climbing, circling behavior, front limb symmetry, and compulsory circling (Wang, et al., 2007). Each test was graded from 0 to 4, establishing a maximum deficit score of 24.

2.5. Brain swelling, lesion volume, tissue loss, and ventricular expansion

Mice were euthanized after the neurologic examination on day 3 or 28 post-ICH. The entire brain of each mouse was cut into 50-μm sections at 10 rostral-caudal levels that were spaced 360 μm apart. The sections were stained with Luxol fast blue (for myelin) and Cresyl Violet (for neurons) before being quantified for brain swelling and lesion volume with SigmaScan Pro software (version 5.0.0 for Windows; Systat, San Jose, CA) (H. Wu, et al., 2011). The lesion volume in cubic millimeters was calculated by multiplying the section thickness by the damaged areas of each section and was corrected for brain swelling: corrected lesion volume = volume of non-hemorrhagic hemisphere – (volume of hemorrhagic hemisphere – lesion volume). The volume of tissue lost and ventricular expansion on day 28 after ICH was determined as described previously (Wasserman, et al., 2008). The volume of tissue lost was the difference between the volume of the contralateral striatum and the remaining volume of the ipsilateral striatum, and the volume of ventricular expansion was the difference between the volume of the ipsilateral and contralateral ventricles.

2.6. Brain water content

The extent of brain edema after ICH was determined by brain water content measurement on day 3 after ICH. The brains were removed and dissected into ipsilateral and contralateral striatum and cerebellum (which served as an internal control). The percentage of brain water content was calculated as: (wet weight – dry weight) / wet weight00D7;100% (Wu, et al., 2012).

2.7. Spectrophotometric assay for hemoglobin

Drabkin’s reagent (Sigma) was used to quantify the hemoglobin content of brains at 24 hours after collagenase-induced ICH, as described previously (Wang, et al., 2003). The brain tissue was trimmed to contain only the striatum. The concentration of cyanomethemoglobin in the homogenates of striatal tissue was measured spectrophotometrically at 540 nm.

2.8. Histology

Fluoro-Jade B (FJB) was used to quantify neuronal death (Wang and Tsirka, 2005a; Xue, et al., 2009a). To quantify FJB-positive cells in the perihematomal region along the rostral-caudal axis, we selected three sections each from mice with similar lesion areas (at the injection site and 360 μm to each side) to target similar regions of interest. The perihematomal region that was examined lies within 200 μm of the lesion border. FJB-

positive cells were quantified in the lateral edge of the hematoma in the caudate putamen. The numbers of FJB-positive cells from 12 locations per mouse (4 fields per section × 3 sections per mouse) were averaged and expressed as positive cells per square millimeter (30× magnification; n=8 mice/group).

2.9. Immunofluorescence

Immunofluorescence (n=8 mice/group) was carried out as we have described previously (Wang and Tsirka, 2005a). Primary antibodies used were: rabbit antimyeloperoxidase (MPO, neutrophil marker; 1:500; Dako, Carpinteria, CA); rabbit anti-Iba 1 (microglia/macrophage marker; 1:500; Wako Chemicals, Richmond, VA); rabbit anti-NeuN (neuronal marker; 1:500; Dako, Carpinteria, CA); and rabbit anti-glial fibrillary acidic protein (GFAP, astrocyte marker; 1:500; Dako). Sections were then incubated with Alexa 488-conjugated goat anti-rabbit secondary antibody (1:1000; Molecular Probes, Eugene, OR). Stained sections were examined with a fluorescence microscope (ECLIPSE TE2000-E, Nikon, Japan). In selected sections with similar lesion areas, cells that were immunoreactive for Iba1, GFAP, and MPO were quantified as described above under a 40× objective. After ICH, activated microglia/macrophages were defined as cells with a cell body more than 7.5 μm in at least one direction, with short, thick processes and intense immunoreactivity. Resting microglia were characterized by small cell bodies (<7.5 μm in all directions), long processes, and weak immunoreactivity. By using this combination of morphologic criteria, we defined microglia/macrophages as either resting or activated (Wang, et al., 2008).

2.10. Gelatin in situ and gel zymography

In situ gelatinolytic activity was detected on fresh frozen brain sections (Wang and Tsirka, 2005a). Sections were incubated in reaction buffer with 40 μg/mL DQ– gelatin-FITC (Invitrogen, Carlsbad, CA) at 37°C for 1 hour and washed and fixed in 4% paraformaldehyde in phosphate-buffered saline. Cleavage of DQ–gelatin-FITC by gelatinase results in a green fluorescent product (excitation, 495 nm; emission, 515 nm). To quantify gelatinolytic activity-positive cells, we focused on areas adjacent to the hematoma and applied a strategy similar to that described above.

Prepared protein samples (500 μg) from whole hemorrhagic hemispheres were loaded and separated on a 10% gelatin zymogram gel (Invitrogen) as we have described previously (Wang and Tsirka, 2005a). A mixture of mouse pro-MMP-9 (98 kDa) and pro-MMP-2 (72 kDa) (R&D Systems, Minneapolis, MN) was used as the gelatinase standard. After separation, the gel was incubated in renaturing buffer (2.5% Triton X-100) twice for 1 hour at room temperature with gentle agitation and then with developing buffer (50 mM Tris-HCl [pH 7.5], 200 mM NaCl, 5 mM $CaCl_2$, 0.05% Brij-35, 0.02% NaN_3). The gel was then stained with 0.5% Coomassie blue R-250 for 30 minutes and destained appropriately to be photographed (FluorChem HD2, Alpha Innotech, San Leandro, CA). Gels were analyzed densitometrically (ImageJ, National Institutes of Health, Bethesda, MD, USA) on coded samples. MMP-2/9 activity was measured by optical density and quantified as fold increase compared with sham controls. We examined five brains per group.

2.11. Western blotting

Brain tissue from the whole hemorrhagic hemisphere was obtained 24 hours after ICH. Twenty-microgram protein samples were separated by 4–12% sodium dodecyl sulfate polyacrylamide gel electrophoresis and transferred onto polyvinylidene difluoride membranes. The membranes were probed with the following primary antibodies: rabbit anti-HMGB1 (1:500, Abcam, Cambridge, MA), rabbit anti-Src (1:1000, Cell Signaling Technology, Danvers, MA), rabbit anti-phospho-Src (Tyr416, 1:1000, Cell Signaling), rabbit anti-cyclooxygenase (COX)-2 (1:100, Cayman Chemical, Ann Arbor, MI), rabbit anti-interleukin (IL)-1β (1:200, Abcam), and rabbit anti-β-actin (1:5000, Abcam). Resulting protein bands were scanned and analyzed with ImageJ software. Data were expressed as fold change over the loading control. We examined five brains per treatment group and three brains per sham group.

2.12. In situ detection of reactive oxygen species

Production of superoxide was investigated by in situ detection of oxidized hydroethidine (Park, et al., 2007; Wang and Tsirka, 2005a). Hydroethidine, a cell-permeable oxidative fluorescent dye, is oxidized by superoxide to ethidium, which intercalates within the DNA and emits a red fluorescent signal. This method provides sensitive detection of superoxide levels in situ. The fresh brain sections were washed with phosphate-buffered saline (PBS) and incubated with hydroethidine (10 μM) in PBS for 30 minutes at 37°C. Fluorescence intensity was determined in the perihematomal region (at the injection site and at 360 μm to each side) after subtraction of the color density on the contralateral striatum (n=5 mice/group). For quantification of fluorescent intensity, all images were captured at the same intensity, contrast settings, and exposure times and analyzed by ImageJ software on coded samples. Immunofluorescence staining with NeuN antibody was also performed on some of these brain sections (n=5 mice).

2.13. Protein oxidation assay

Oxidative modification of proteins in striatum after ICH was determined with an OxyBlot protein oxidation detection kit (Millipore, Billerica, MA) according to the manufacturer's instructions. OxyBlot analysis identifies protein carbonyl groups, a hallmark of the oxidative alteration of proteins. Aliquots of equal amounts of protein (20 μg) were denatured with 10% sodium dodecyl sulfate (SDS) and then derivatized to 2,4-dinitrophenylhydrazone (DNP) by a reaction with 2,4-dinitrophenylhydrazine (DNPH) for 5 minutes. This reaction allows for a chemical conjugation of DNPH to the carbonyl group of the protein side chain to create a hydrazone moiety that can be detected by immunochemistry. The reaction was quenched with a neutralizing solution that caused a color change to brown. Samples were then placed on ice and loaded onto 4–12% SDS polyacrylamide gels for protein separation by electrophoresis. Proteins with conjugated DNP residues were detected with polyclonal rabbit antibody to DNP (diluted 1:150). Proteins were then incubated with horseradish peroxidase-conjugated goat anti-rabbit IgG antibody (1:300) and visualized by enhanced chemiluminescence and exposure to radiographic film. Optical density values were normalized to the corresponding loading control on each gel and were expressed as fold change over that of sham-operated mice. We examined five brains per group.

2.14. Statistics

Parametric data are expressed as means ± SD. Differences between two groups were determined by two-tailed Student's *t*-test. The statistical comparisons among multiple groups were made by using one-way ANOVA followed by Bonferroni correction. A Chi-square test was used for analyzing mortality. For mouse body weight changes, we applied repeated measures ANOVA to compare differences between treatment groups over time. Power calculation was performed based on sample size, means, and standard deviation of the means. Statistical significance was set at $p<0.05$.

3. Results

3.1. Misoprostol treatment decreases brain lesion volume, edema, and tissue loss and improves long-term neurologic outcome

Mice were subjected to the collagenase-induced ICH model in the primary study and the blood ICH model in the secondary study. In both ICH models, misoprostol treatment reduced lesion volume (both $p<0.05$, n = 8–11 mice/group) and brain water content (both $p<0.05$, n = 5 mice/group) on day 3 (Fig. 1A and B) and volume of tissue loss (both $p<0.05$, n = 6–8 mice/group) on day 28 after ICH (Fig. 2A and B). Misoprostol treatment also decreased the volume of ventricular expansion; however, the difference was not significant (both $p>0.05$, n = 6–8 mice/group; Fig. 2A and B).

Compared with baseline values, neurologic deficits were apparent in all mice subjected to ICH, regardless of model. Neurologic deficit scores were lower in misoprostol-treated mice than in vehicle-treated mice on day 28 ($p<0.01$), but not on day 3 after ICH ($p>0.05$, n = 6–8 mice/group; Fig. 2A and B). In the collagenase ICH model, power analysis showed a power of 92.3% to detect a significant difference in corrected lesion volume on day 3 and a power of 95% to detect a significant difference in neurologic deficit score on day 28 after ICH. In the blood ICH model, power analysis showed a power of 81.2% to detect a significant difference in corrected lesion volume on day 3 and a power of 75.8% to detect a significant difference in neurologic deficit score on day 28 after ICH. The results suggest that the efficacy of misoprostol is not animal-model dependent.

3.2. Mortality and body weight changes

In the collagenase-induced ICH model, the mortality of misoprostol-treated mice (15.0%, 6/40) was not different from that of vehicle-treated mice (9.4%, 3/32; $p>0.05$). Similarly, in the blood ICH model, the mortality of misoprostol-treated mice (13.0%, 3/23) was not different from that of vehicle-treated mice (23.1%, 6/26; $p>0.05$). Most deaths occurred within 24 hours after ICH. No animals died in any of the sham groups (0 of 9).

In the collagenase-induced ICH model, mouse body weight was decreased compared to baseline during the first week after ICH. Body weight of mice treated with misoprostol or vehicle recovered after day 3 and matched each other from day 7 onward ($F=4.212$, $p=0.06$, n=8 mice/group; Supplemental Fig. 1A). Mice subjected to the blood ICH model also lost weight within the first 3 days after ICH. Body weight loss of mice treated with misoprostol

and vehicle did not differ after ICH (F=9.29, p>0.05, n=6 mice/group; Supplemental Fig. 1B).

3.3. Misoprostol treatment decreases neuronal death in the collagenase-induced ICH model

FJB staining showed that degenerating neurons were distributed equally around the hematoma on day 3 after collagenase-induced ICH. Misoprostol treatment reduced the number of FJB-positive cells by 59.9% in the peri-ICH area on day 3 after ICH (p<0.01, n=8 mice/group; Fig. 3A).

3.4. Misoprostol treatment has no effect on collagenase-induced bleeding

To exclude the possibility that the misoprostol-induced reduction in brain injury resulted from decreased collagenase-induced bleeding, we measured the initial levels of hemoglobin content in the injured striatum. No difference between misoprostol- and vehicle-treated mice was observed 24 hours after ICH (n=6 mice/group, p>0.05, Fig. 3B), indicating that misoprostol treatment does not affect collagenase-induced bleeding.

3.5. Misoprostol treatment decreases cellular inflammatory response in the collagenase model

Microglial/macrophage activation contributes to ICH-induced early brain injury (Wang, 2010). To examine the effect of misoprostol treatment on microglial/macrophage activation after ICH, we used Iba1 immunofluorescence labeling. Misoprostol treatment reduced the number of activated microglia/macrophages in the peri-ICH area on day 3 after ICH (p<0.05, n = 8 mice/group; Fig. 4A and B). At a lower magnification, Iba1 labeling shows that activated microglia/macrophages were distributed equally around the hematoma on day 3 after collagenase-induced ICH (Fig. 4C).

To examine the effect of misoprostol treatment on astrocyte reactivity, we used GFAP immunofluorescence labeling. Compared with resting astrocytes, reactive astrocytes in the perihematomal region exhibited intense GFAP immunoreactivity and a greater number, length, and thickness of GFAP-positive processes. We found that misoprostol treatment reduced the number of reactive astrocytes in the peri-ICH area on day 3 after ICH (p<0.05, n = 8 mice/group; Fig. 4A and B). At a lower magnification, GFAP labeling shows that reactive astrocytes were distributed equally around the hematoma on day 3 after collagenase-induced ICH (Fig. 4C).

Neutrophil infiltration occurs after early activation of microglia/macrophages and contributes to early hemorrhagic brain injury (Moxon-Emre and Schlichter, 2011; Wang, 2010). To examine the effect of misoprostol on neutrophil infiltration, we used MPO immunofluorescence labeling. MPO-immunoreactive neutrophils were evident in the peri-ICH area on day 3 after ICH. Misoprostol treatment reduced their number (p<0.01, n = 8 mice/group; Fig. 4A and B).

3.6. Misoprostol treatment attenuates superoxide production and protein oxidation in the collagenase model

Oxidative stress in the brain can cause neuronal death (Wang and Dore, 2007). We used the fluorescent indicator hydroethidine to study the effect of misoprostol treatment on superoxide production. In misoprostol-treated mice, superoxide production measured by dihydroethidium fluorescence intensity (ethidium signals, small red particles) was markedly attenuated in the peri-ICH area on day 1 after ICH ($p<0.01$, n = 5 mice/group; Fig. 5A and B). We further confirmed that increased ethidium signals were mostly detected in NeuN-positive neuronal nucleus (n = 5 mice; Fig. 5C).

OxyBlot analysis indicated significant oxidative alteration to proteins at 24 hours after ICH. Proteins between 29 and 98 kDa appeared to be prominent targets of oxidative stress. The intensity of these bands was elevated at 24 hours after ICH. Treatment with misoprostol reduced carbonyl formation on day 1 after ICH ($F = 8.241$, $p<0.05$, n = 5 mice/group; Fig. 5D and E).

3.7. Misoprostol treatment decreases gelatinolytic activity in the collagenase model

We and others have shown previously that increased gelatinolytic activity (MMP-2/9) contributes to ICH-induced brain damage (Wang and Tsirka, 2005a; Xue, et al., 2006). Using in situ zymography, we compared gelatinolytic activity in the perihematomal region of mice treated with misoprostol to that of mice treated with vehicle. As we have reported, gelatinolytic activity was associated mostly with neuronlike cells (Wang and Tsirka, 2005a). Misoprostol treatment decreased gelatinolytic activity in the perihematomal region compared with that of vehicle-treated controls on day 1 after ICH ($p<0.01$, n=5 mice/group; Fig. 6A and B). Consistent with these findings, gelatin gel zymography revealed a decrease in the intensity of pro-MMP-9 (98 kDa) and pro-MMP-2 (72 kDa) bands in hemorrhagic brains of misoprostol-treated mice on day 1 after ICH. ($p<0.01$, n=5 mice/group; Fig. 6C and D). The active MMP-2/9 bands were not reliably detectable, consistent with previous reports (Rosell, et al., 2006; Xue, et al., 2006).

3.8. Misoprostol treatment decreases HMGB1 expression, Src phosphorylation (Tyr416), and IL-1β expression in the collagenase model

Proinflammatory factors HMGB1 and COX-2, cytokine IL-1β, and Src kinase activation all contribute to ICH-induced secondary brain injury (Ardizzone, et al., 2007; Chu, et al., 2004; Ohnishi, et al., 2011; Wang and Dore, 2007). Therefore, we investigated whether misoprostol treatment regulates protein expression of HMGB1, COX-2, or IL-1β or activity of Src, which can be ascertained by its level of phosphorylation at Tyr416 (Roskoski, 2004). Western blot analysis showed that expression levels of HMGB1, COX-2, IL-1β, and phospho-Src were markedly increased on day 1 after ICH (Fig. 7). Misoprostol reduced the expression of HMGB1, phospho-Src, and IL-1β ($F = 22.122$, 20.424, 78.817, respectively, $p<0.05$, $p<0.01$, n=5 mice/group; Fig. 7A, B, and D) but did not reduce COX-2 expression ($F = 13.243$, $p>0.05$, n=5 mice/group; Fig. 7C).

3.9. HMGB1 inhibition decreases Src phosphorylation (Tyr416), MMP-9 activity, neuronal death, and brain lesion volume in the collagenase model

Because misoprostol decreases HMGB1 expression, we investigated whether HMGB1 inhibition protects against ICH-induced brain injury. When cells become injured or undergo necrosis, HMGB1, which normally resides in the nucleus, translocates to the cytoplasm and/or extracellular space. We first examined HMGB1 expression after collagenase-induced ICH. HMGB1 staining in the contralateral striatum was unchanged at 5 and 24 hours after ICH, but decreased at 72 hours. However, the number of HMGB1-positive cells in the perihematomal region was increased compared with that in sham animals (Supplemental Fig. 2). To identify the cell types in which HMGB1 was expressed after ICH, we double labeled brain sections with anti-HMGB1 and anti-NeuN antibodies (Supplemental Fig. 2). HMGB1 immunoreactivity was associated mostly with neurons, suggesting that neurons are selectively vulnerable to ICH and could be one of the main sources of released HMGB1 at early post-ICH time points.

Glycyrrhizin, a component of licorice root, has been shown to bind directly to HMGB1 and inhibit its cytokine-like activity (Girard, 2007; Mollica, et al., 2007). We found that glycyrrhizin markedly decreased HMGB1 expression at 24 hours after ICH ($F = 21.665$, $p<0.05$, n=5 mice/group; Fig. 8A), confirming that it is a potent inhibitor of HMGB1. Furthermore, we found that HMGB1 inhibition with glycyrrhizin decreased Src phosphorylation (Tyr416) and MMP-9 activity ($F = 27.408$, 82.156, respectively, both $p<0.01$) at 24 hours after ICH (n=5 mice/group; Fig. 8B and C), decreased neuronal death ($p<0.01$) as assessed by FJB-staining at 24 hours (n=5 mice/group; Fig. 8D), and decreased brain swelling and lesion volume (both $p<0.05$) on day 3 after ICH (n=8 mice/group; Fig. 8E).

3.10. Src kinase inhibition decreases MMP-9 activity and brain edema and improves neurologic function in the collagenase model

Src kinase inhibition is protective in a blood-induced ICH rat model (Ardizzone, et al., 2007). Because misoprostol decreases Src kinase activity, we examined whether Src kinase inhibition is also protective in the collagenase-induced ICH mouse model. We found that Src kinase inhibitor PP2 blocked increases in Src phosphorylation at Tyr416 ($p<0.05$, n=5 mice/group; Fig. 9A) but did not affect HMGB1 protein levels ($F = 11.635$, $p>0.05$, n=5 mice/group; Fig. 9B). It also decreased MMP-9 activity ($F = 25.007$, $p<0.01$, n=5 mice/group; Fig. 9E) on day 1 after ICH and decreased brain water content ($p<0.01$, n=6 mice/group; Fig. 9C) and neurologic deficit score ($p<0.01$, n=6 mice/group; Fig. 9D) on day 3 after ICH.

4. Discussion

Misoprostol binds to the EP2 and EP4 receptors and increases cAMP production, indicating that it is an agonist of these receptors (Jones, et al., 2009; Reimer, et al., 1992). Previous studies have shown that misoprostol protects brain against cerebral ischemia (Li, et al., 2008; Taniguchi, et al., 2011). We demonstrated here that misoprostol is also protective in two ICH models and confirmed its efficacy in two independent laboratories. Our study

presents several novel findings: 1) post-treatment with misoprostol decreases brain lesion volume, edema, neuronal death, brain atrophy, and long-term neurologic function up to day 28 but does not affect collagenase-induced bleeding; 2) post-treatment with misoprostol decreases cellular inflammatory response and attenuates superoxide production and protein oxidation; 3) post-treatment with misoprostol decreases HMGB1 expression, Src phosphorylation, IL-1β expression, and gelatinolytic activity; 4) post-treatment with misoprostol does not increase mortality rate or weight loss; 5) HMGB1 inhibition decreases Src phosphorylation (Tyr416), MMP-9 activity, neuronal death, and brain lesion volume; and 6) Src kinase inhibition does not decrease HMGB1 protein levels, but decreases MMP-9 activity, brain edema, and neurologic deficit score. Together, these observations suggest that misoprostol can protect brain against ICH injury through mechanisms that may involve the HMGB1, Src kinase, and MMP-2/9 pathway.

Inflammation contributes to secondary brain injury after ICH. The cellular inflammatory responses involve activation of microglia and astrocytes and infiltration of neutrophils and macrophages. A molecular response follows that involves release of inflammatory mediators, including cytokines, reactive oxygen species (ROS), and MMPs (Wang, 2010; Wang and Dore, 2007). Microglia become rapidly activated in response to brain injury and undergo morphologic and molecular changes associated with neurotoxicity. Microglia also were shown to induce ROS production and damage neurons in neuron–microglia co-cultures (Gao, et al., 2003). In ICH models, neutrophil infiltration follows microglia activation (Wang, 2010). Neutrophils are a rich source of MMP-9, which contributes to blood-brain barrier breakdown (Moxon-Emre and Schlichter, 2011). Infiltrating neutrophils die within the first few days after ICH (Wang and Dore, 2007). We and others have shown that inhibition of microglia/macrophage activation (Wang, et al., 2003; Wang and Tsirka, 2005b), depletion of neutrophils (Moxon-Emre and Schlichter, 2011), and inhibition of MMP-2/9 activity (Wang and Tsirka, 2005a; Xue, et al., 2009b) are associated with a decrease in ROS production and are cerebroprotective after ICH.

We showed for the first time that misoprostol treatment decreases cellular responses (microglia/macrophages, neutrophils, and astrocytes) and molecular responses (IL-1β expression, production of superoxide and protein carbonyl groups, and MMP-2/9 activity) of inflammation, confirming that it has anti-inflammatory and antioxidant properties. The decrease in superoxide production in neurons suggests that neurons could be the direct targets of the neuroprotective effect of misoprostol. HMGB1 is newly defined as a cytokine that can be released from necrotic cells in post-ischemic brain (Kim, et al., 2006; Qiu, et al., 2008). Hence, it represents a major upstream paracrine inflammatory mediator within the neurovascular unit (Kim, et al., 2006). Recombinant HMGB1 or HMGB1 released by injured neurons in culture was shown to induce proinflammatory cytokine expression in neurons, astrocytes, and endothelial cells (Qiu, et al., 2008). Anti-HMGB1 neutralizing antibody was shown to protect the blood-brain barrier and ameliorate ischemic stroke injury (Zhang, et al., 2011). As in the ischemic brain (Qiu, et al., 2008), we showed that HMGB1 is expressed mostly in neurons in the perihematomal region at 5 and 24 hours after ICH. Cytokine IL-1β is released primarily from stimulated macrophages and monocytes and plays a key role in the inflammatory response (Shalhoub, et al., 2011). We showed that misoprostol treatment markedly decreases protein expression of HMGB1 and IL-1β at 24

hours after ICH. We and others have shown that COX-2 is upregulated after ICH (Gong, et al., 2001; T. Wu, et al., 2011) and might contribute to inflammation-mediated ICH injury, possibly through excessive PGE2 production (Chu, et al., 2004; Wang and Dore, 2007). However, COX-2 expression was not modified by treatment with misoprostol, excluding COX-2 as a direct target of misoprostol. Because misoprostol might be an agonist of EP2 and EP4 receptors (Jones, et al., 2009; Reimer, et al., 1992), future studies should be carried out to elucidate the role of EP2 and/or EP4 in cerebroprotection conferred by misoprostol.

To further confirm the toxic effect of HMGB1 after ICH, we examined how HMGB1 inhibition with glycyrrhizin affected ICH-related pathogenic events. Consistent with a previous study in rats (Ohnishi, et al., 2011), we found that HMGB1 inhibition is also protective after collagenase-induced ICH in mice. Exogenous HMGB1 upregulates MMP-9 activity in cultured neurons and astrocytes, as well as in mouse brain (Qiu, et al., 2010). Although increased MMP-9 activity contributes to ICH-induced early brain injury (Wang, 2010), it is not clear whether HMGB1 inhibition affects MMP-9 activity. Here, we demonstrated that HMGB1 inhibition with glycyrrhizin decreases MMP-9 activity, thereby decreasing brain injury.

ICH markedly activates Src kinase activity (Ardizzone, et al., 2007). Src-mediated changes in glutamate release, MMP activity, inflammation, and oxidative stress could lead to increases in vascular permeability after ICH (Liu and Sharp, 2011). Src kinase inhibition blocks glutamate release and decreases blood/thrombin-induced brain injury and neuronal death (Ardizzone, et al., 2007; Liu, et al., 2008). Here, we showed that misoprostol decreased Src kinase activity. In ischemic stroke models, Src inhibition decreased edema and infarct size by blocking the vascular permeability effect of vascular endothelial growth factor (Zan, et al., 2011; Zan, et al., 2014). However, the direct response of MMP-9 to Src kinase inhibition has not been established. Using the Src kinase inhibitor PP2, we showed that Src kinase inhibition by PP2 reduces MMP-9 activity, brain water content, and neurologic deficit score in the collagenase-induced ICH model. These neuroprotective effects of PP2 are consistent with those reported in a previous study that used a rat blood ICH model (Ardizzone, et al., 2007). Interestingly, our results also showed that HMGB1 inhibition decreases Src kinase activity, whereas Src kinase inhibitor PP2 does not decrease HMGB1 protein expression, suggesting that Src kinase could be a downstream target of HMGB1.

In conclusion, we have identified an unrecognized cerebroprotective function for the PGE_2 receptor agonist misoprostol in two mouse ICH models from two laboratories. These data indicate that misoprostol may have potentially therapeutic value for patients with ICH, particularly as it is an FDA-approved drug for ulcer prophylaxis and is well tolerated. Our results also suggest that the protective effects of misoprostol could be mediated through mechanisms that involve the HMGB1, Src kinase, and MMP-2/9 pathway. Misoprostol warrants further investigation for potential ICH therapy.

Supplementary Material

Refer to Web version on PubMed Central for supplementary material.

Acknowledgments

This work was supported by AHA 09BGIA2080137, NIH K01AG031926, R01AT007317, R01NS078026 (JW), Foundation of Heilongjiang Province Educational Committee for the Returned Overseas Chinese Scholars 1254HQ004, and the National Natural Science Foundation of China 81200885 (HW). We thank Christine Kim and Francesca di Domenico for blind analysis of histology and immunofluorescence, and Claire Levine and Jiarui Wang for assistance with manuscript preparation.

References

Ardizzone TD, Zhan X, Ander BP, Sharp FR. SRC kinase inhibition improves acute outcomes after experimental intracerebral hemorrhage. Stroke. 2007; 38:1621–1625. [PubMed: 17395859]

Chu K, Jeong SW, Jung KH, Han SY, Lee ST, Kim M, Roh JK. Celecoxib induces functional recovery after intracerebral hemorrhage with reduction of brain edema and perihematomal cell death. J Cereb Blood Flow Metab. 2004; 24:926–933. [PubMed: 15362723]

Cipollone F, Prontera C, Pini B, Marini M, Fazia M, De Cesare D, Iezzi A, Ucchino S, Boccoli G, Saba V, Chiarelli F, Cuccurullo F, Mezzetti A. Overexpression of functionally coupled cyclooxygenase-2 and prostaglandin E synthase in symptomatic atherosclerotic plaques as a basis of prostaglandin E(2)-dependent plaque instability. Circulation. 2001; 104:921–927. [PubMed: 11514380]

Fisher M, Feuerstein G, Howells DW, Hurn PD, Kent TA, Savitz SI, Lo EH. Update of the stroke therapy academic industry roundtable preclinical recommendations. Stroke. 2009; 40:2244–2250. [PubMed: 19246690]

Gao HM, Liu B, Zhang W, Hong JS. Synergistic dopaminergic neurotoxicity of MPTP and inflammogen lipopolysaccharide: relevance to the etiology of Parkinson's disease. Faseb J. 2003; 17:1957–1959. [PubMed: 12923073]

Girard JP. A direct inhibitor of HMGB1 cytokine. Chem Biol. 2007; 14:345–347. [PubMed: 17462568]

Gong C, Ennis SR, Hoff JT, Keep RF. Inducible cyclooxygenase-2 expression after experimental intracerebral hemorrhage. Brain Res. 2001; 901:38–46. [PubMed: 11368948]

Grossetete M, Rosenberg GA. Matrix metalloproteinase inhibition facilitates cell death in intracerebral hemorrhage in mouse. J Cereb Blood Flow Metab. 2008; 28:752–763. [PubMed: 17971790]

Hurn PD, Vannucci SJ, Hagberg H. Adult or perinatal brain injury: does sex matter? Stroke. 2005; 36:193–195. [PubMed: 15625289]

Jones RL, Giembycz MA, Woodward DF. Prostanoid receptor antagonists: development strategies and therapeutic applications. Br J Pharmacol. 2009; 158:104–145. [PubMed: 19624532]

Kim JB, Sig Choi J, Yu YM, Nam K, Piao CS, Kim SW, Lee MH, Han PL, Park JS, Lee JK. HMGB1, a novel cytokine-like mediator linking acute neuronal death and delayed neuroinflammation in the postischemic brain. J Neurosci. 2006; 26:6413–6421. [PubMed: 16775128]

Li J, Liang X, Wang Q, Breyer RM, McCullough L, Andreasson K. Misoprostol, an anti-ulcer agent and PGE2 receptor agonist, protects against cerebral ischemia. Neurosci Lett. 2008; 438:210–215. [PubMed: 18472336]

Liang X, Lin L, Woodling NS, Wang Q, Anacker C, Pan T, Merchant M, Andreasson K. Signaling via the prostaglandin E receptor EP4 exerts neuronal and vascular protection in a mouse model of cerebral ischemia. J Clin Invest. 2011; 121:4362–4371. [PubMed: 21965326]

Liu D, Wu L, Breyer R, Mattson MP, Andreasson K. Neuroprotection by the PGE2 EP2 receptor in permanent focal cerebral ischemia. Ann Neurol. 2005; 57:758–761. [PubMed: 15852374]

Liu DZ, Cheng XY, Ander BP, Xu H, Davis RR, Gregg JP, Sharp FR. Src kinase inhibition decreases thrombin-induced injury and cell cycle re-entry in striatal neurons. Neurobiol Dis. 2008; 30:201–211. [PubMed: 18343677]

Liu DZ, Sharp FR. The dual role of SRC kinases in intracerebral hemorrhage. Acta Neurochir Suppl. 2011; 111:77–81. [PubMed: 21725735]

McCullough L, Wu L, Haughey N, Liang X, Hand T, Wang Q, Breyer RM, Andreasson K. Neuroprotective function of the PGE2 EP2 receptor in cerebral ischemia. J Neurosci. 2004; 24:257–268. [PubMed: 14715958]

Mollica L, De Marchis F, Spitaleri A, Dallacosta C, Pennacchini D, Zamai M, Agresti A, Trisciuoglio L, Musco G, Bianchi ME. Glycyrrhizin binds to high-mobility group box 1 protein and inhibits its cytokine activities. Chem Biol. 2007; 14:431–441. [PubMed: 17462578]

Moxon-Emre I, Schlichter LC. Neutrophil depletion reduces blood-brain barrier breakdown, axon injury, and inflammation after intracerebral hemorrhage. J Neuropathol Exp Neurol. 2011; 70:218–235. [PubMed: 21293296]

Numo R. Prevention of NSAID-induced ulcers by the coadministration of misoprostol: implications in clinical practice. Scand J Rheumatol Suppl. 1992; 92:25–29. [PubMed: 1574685]

Ohnishi M, Katsuki H, Fukutomi C, Takahashi M, Motomura M, Fukunaga M, Matsuoka Y, Isohama Y, Izumi Y, Kume T, Inoue A, Akaike A. HMGB1 inhibitor glycyrrhizin attenuates intracerebral hemorrhage-induced injury in rats. Neuropharmacology. 2011; 61:975–980. [PubMed: 21752338]

Park L, Anrather J, Girouard H, Zhou P, Iadecola C. Nox2-derived reactive oxygen species mediate neurovascular dysregulation in the aging mouse brain. J Cereb Blood Flow Metab. 2007; 27:1908–1918. [PubMed: 17429347]

Qiu J, Nishimura M, Wang Y, Sims JR, Qiu S, Savitz SI, Salomone S, Moskowitz MA. Early release of HMGB-1 from neurons after the onset of brain ischemia. J Cereb Blood Flow Metab. 2008; 28:927–938. [PubMed: 18000511]

Qiu J, Xu J, Zheng Y, Wei Y, Zhu X, Lo EH, Moskowitz MA, Sims JR. High-mobility group box 1 promotes metalloproteinase-9 upregulation through Toll-like receptor 4 after cerebral ischemia. Stroke. 2010; 41:2077–2082. [PubMed: 20671243]

Reimer R, Heim HK, Muallem R, Odes HS, Sewing KF. Effects of EP-receptor subtype specific agonists and other prostanoids on adenylate cyclase activity of duodenal epithelial cells. Prostaglandins. 1992; 44:485–493. [PubMed: 1361678]

Rosell A, Ortega-Aznar A, Alvarez-Sabin J, Fernandez-Cadenas I, Ribo M, Molina CA, Lo EH, Montaner J. Increased brain expression of matrix metalloproteinase-9 after ischemic and hemorrhagic human stroke. Stroke. 2006; 37:1399–1406. [PubMed: 16690896]

Roskoski R Jr. Src protein-tyrosine kinase structure and regulation. Biochem Biophys Res Commun. 2004; 324:1155–1164. [PubMed: 15504335]

Shalhoub J, Falck-Hansen MA, Davies AH, Monaco C. Innate immunity and monocyte-macrophage activation in atherosclerosis. J Inflamm (Lond). 2011; 8:9. [PubMed: 21526997]

Taniguchi H, Anacker C, Suarez-Mier GB, Wang Q, Andreasson K. Function of prostaglandin E2 EP receptors in the acute outcome of rodent hypoxic ischemic encephalopathy. Neurosci Lett. 2011; 504:185–190. [PubMed: 21939736]

Wang J. Preclinical and clinical research on inflammation after intracerebral hemorrhage. Prog Neurobiol. 2010; 92:463–477. [PubMed: 20713126]

Wang J, Dore S. Inflammation after intracerebral hemorrhage. J Cereb Blood Flow Metab. 2007; 27:894–908. [PubMed: 17033693]

Wang J, Fields J, Dore S. The development of an improved preclinical mouse model of intracerebral hemorrhage using double infusion of autologous whole blood. Brain Res. 2008; 1222:214–221. [PubMed: 18586227]

Wang J, Fields J, Zhao C, Langer J, Thimmulappa RK, Kensler TW, Yamamoto M, Biswal S, Dore S. Role of Nrf2 in protection against intracerebral hemorrhage injury in mice. Free Radic Biol Med. 2007; 43:408–414. [PubMed: 17602956]

Wang J, Rogove AD, Tsirka AE, Tsirka SE. Protective role of tuftsin fragment 1–3 in an animal model of intracerebral hemorrhage. Ann Neurol. 2003; 54:655–664. [PubMed: 14595655]

Wang J, Tsirka SE. Neuroprotection by inhibition of matrix metalloproteinases in a mouse model of intracerebral haemorrhage. Brain. 2005a; 128:1622–1633. [PubMed: 15800021]

Wang J, Tsirka SE. Tuftsin fragment 1–3 is beneficial when delivered after the induction of intracerebral hemorrhage. Stroke. 2005b; 36:613–618. [PubMed: 15692122]

Wasserman JK, Yang H, Schlichter LC. Glial responses, neuron death and lesion resolution after intracerebral hemorrhage in young vs. aged rats. Eur J Neurosci. 2008; 28:1316–1328. [PubMed: 18973558]

Wu H, Wu T, Li M, Wang J. Efficacy of the lipid-soluble iron chelator 2,2'-dipyridyl against hemorrhagic brain injury. Neurobiol Dis. 2012; 45:388–394. [PubMed: 21930208]

Wu H, Wu T, Xu X, Wang J, Wang J. Iron toxicity in mice with collagenase-induced intracerebral hemorrhage. J Cereb Blood Flow Metab. 2011; 31:1243–1250. [PubMed: 21102602]

Wu H, Zhang Z, Hu X, Zhao R, Song Y, Ban X, Qi J, Wang J. Dynamic changes of inflammatory markers in brain after hemorrhagic stroke in humans: a postmortem study. Brain Res. 2010; 1342:111–117. [PubMed: 20420814]

Wu T, Wu H, Wang J, Wang J. Expression and cellular localization of cyclooxygenases and prostaglandin E synthases in the hemorrhagic brain. J Neuroinflammation. 2011; 8:22. [PubMed: 21385433]

Xue M, Fan Y, Liu S, Zygun DA, Demchuk A, Yong VW. Contributions of multiple proteases to neurotoxicity in a mouse model of intracerebral haemorrhage. Brain. 2009a; 132:26–36. [PubMed: 18772219]

Xue M, Hollenberg MD, Demchuk A, Yong VW. Relative importance of proteinase-activated receptor-1 versus matrix metalloproteinases in intracerebral hemorrhage-mediated neurotoxicity in mice. Stroke. 2009b; 40:2199–2204. [PubMed: 19359644]

Xue M, Hollenberg MD, Yong VW. Combination of thrombin and matrix metalloproteinase-9 exacerbates neurotoxicity in cell culture and intracerebral hemorrhage in mice. J Neurosci. 2006; 26:10281–10291. [PubMed: 17021183]

Zan L, Wu H, Jiang J, Zhao S, Song Y, Teng G, Li H, Jia Y, Zhou M, Zhang X, Qi J, Wang J. Temporal profile of Src, SSeCKS, and angiogenic factors after focal cerebral ischemia: correlations with angiogenesis and cerebral edema. Neurochem Int. 2011; 58:872–879. [PubMed: 21334414]

Zan L, Zhang X, Xi Y, Wu H, Song Y, Teng G, Li H, Qi J, Wang J. Src regulates angiogenic factors and vascular permeability after focal cerebral ischemia-reperfusion. Neuroscience. 2014; 262:118–128. [PubMed: 24412374]

Zhang J, Takahashi HK, Liu K, Wake H, Liu R, Maruo T, Date I, Yoshino T, Ohtsuka A, Mori S, Nishibori M. Anti-high mobility group box-1 monoclonal antibody protects the blood-brain barrier from ischemia-induced disruption in rats. Stroke. 2011; 42:1420–1428. [PubMed: 21474801]

Zhou Y, Xiong KL, Lin S, Zhong Q, Lu FL, Liang H, Li JC, Wang JZ, Yang QW. Elevation of high-mobility group protein box-1 in serum correlates with severity of acute intracerebral hemorrhage. Mediators Inflamm. 2010:142458. 2010. [PubMed: 20936104]

Highlights

- We examined the efficacy of misoprostol after ICH in 12-month-old mice.
- Post-treatment was protective in the collagenase and blood ICH models.
- Post-treatment reduced HMGB1 expression, Src kinase and MMP-2/9 activity.
- Inhibition of HMGB1 or Src kinase activity was also protective in the ICH model.
- Misoprostol could protect brain against ICH injury.

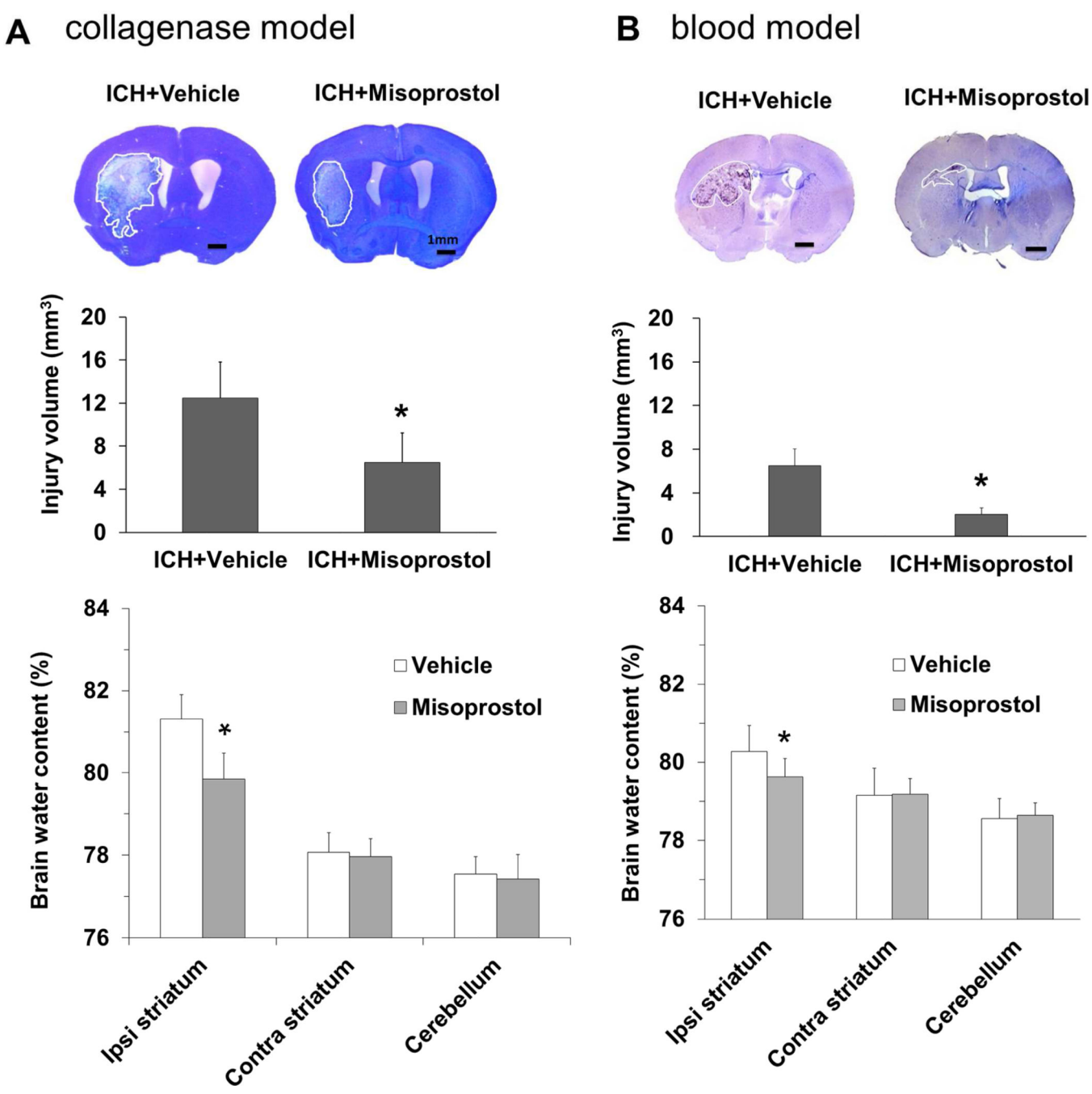

Fig. 1.

Misoprostol treatment decreases brain lesion volume, edema, and neurologic deficits on day 3 after ICH. Representative images of Luxol fast blue/Cresyl Violet-stained brain sections on day 3 after ICH in the collagenase model (**A, top**) and in the blood model (**B, top**). The lesion area, circled in white, is indicated by a lack of staining. Brain lesion volume, which was corrected for brain swelling, was smaller in the misoprostol-treated group than in the vehicle-treated group in the collagenase model (n = 11 mice/group, **A, middle**) and in the blood model (n = 8 mice/group, **B, middle**). Brain water content was less in striatum of misoprostol-treated mice than in striatum of vehicle-treated mice in the collagenase model

(n=5 mice/group, **A, bottom**) and in the blood model (n = 5 mice/group, **B, bottom**). Scale bars: 1 mm. All values are means ± SD; *p<0.05, **p<0.01, t-test.

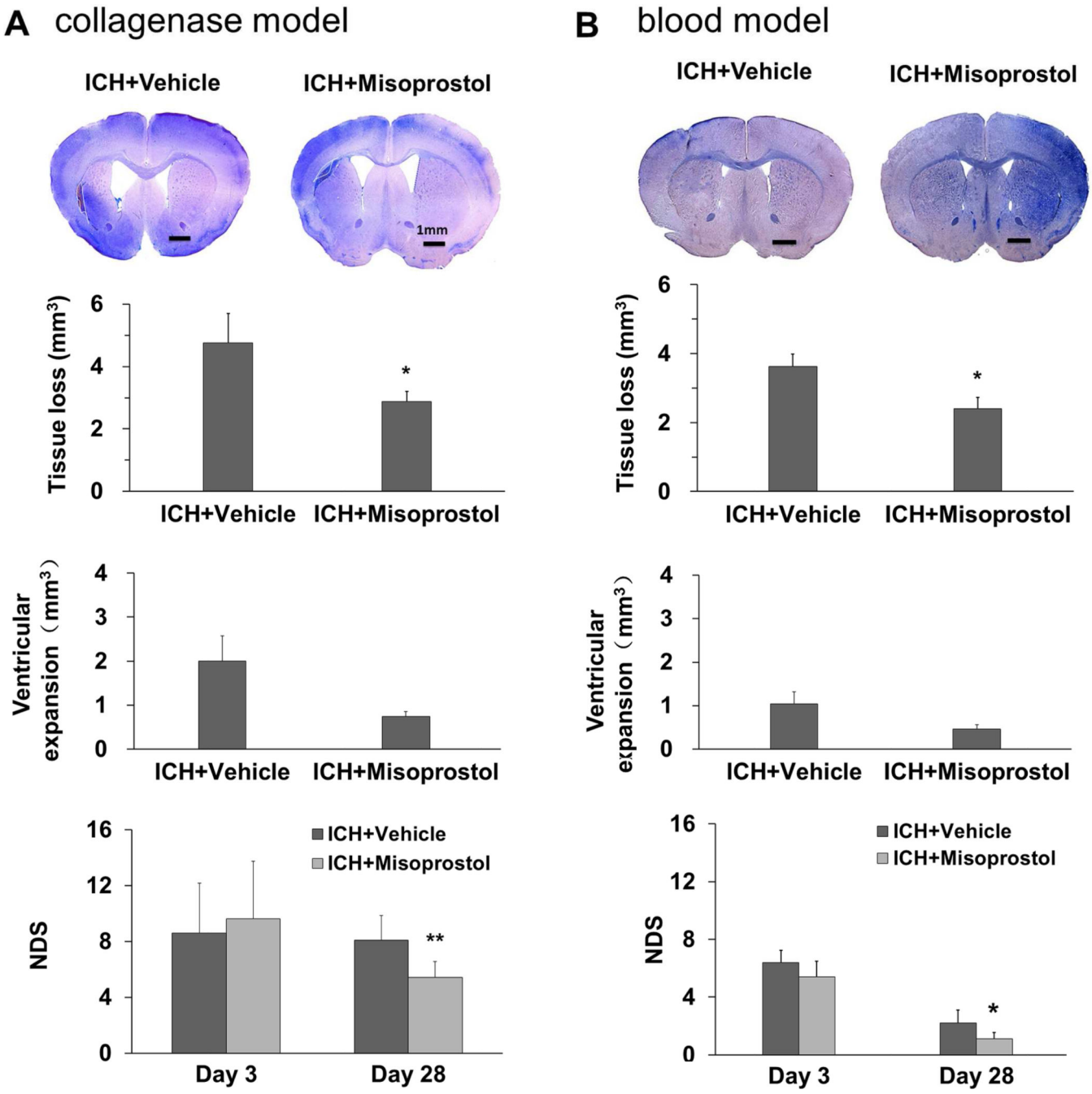

Fig. 2.

Misoprostol treatment decreases brain tissue loss, ventricular expansion, and neurologic deficits on day 28 after ICH. Representative images of Luxol fast blue/Cresyl Violet-stained brain sections on day 28 after ICH in the collagenase model (**A, top**) and in the blood model (**B, top**). Residual lesion, circled in white, can be clearly observed in the collagenase model. Compared with vehicle treatment, misoprostol treatment decreased volume of brain tissue loss and ventricular expansion in both models. Misoprostol also ameliorated neurologic deficit score (NDS) on day 28, but not on day 3, after ICH in the collagenase model (n = 8

mice/group, **A**) and blood model (n = 6 mice/group, **B**). Scale bars: 1 mm. All values are means ± SD; *p<0.05, **p<0.01, t-test.

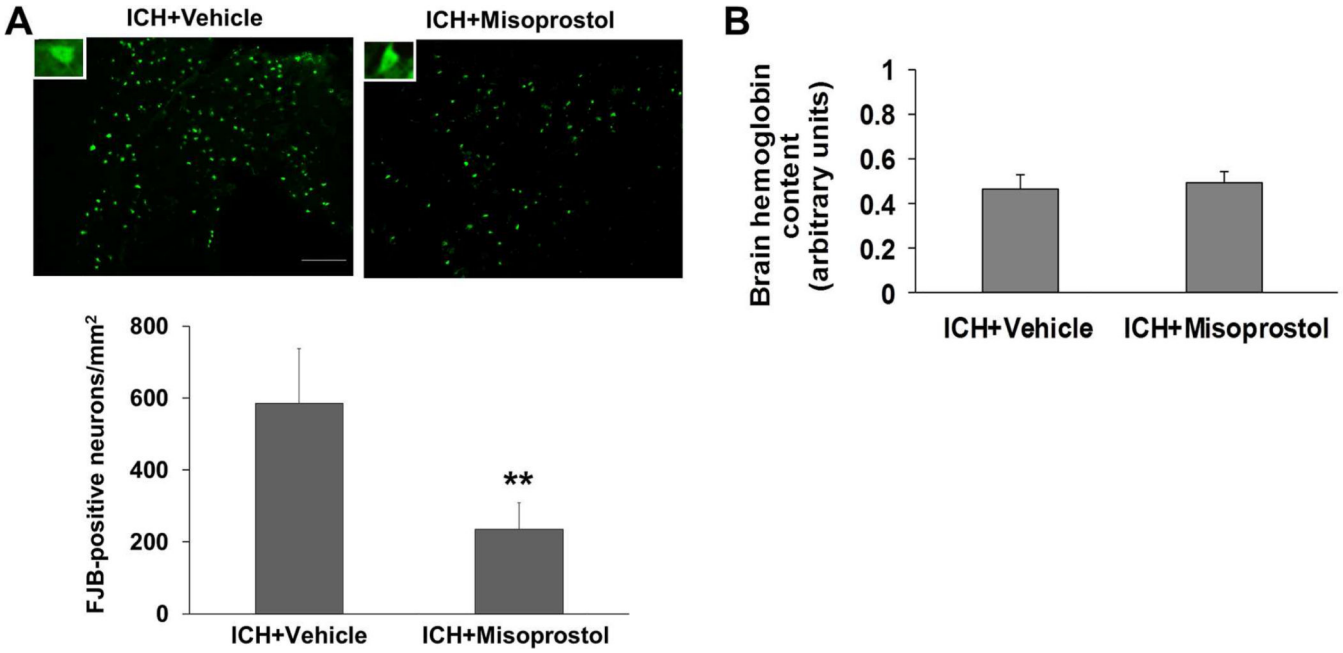

Fig. 3.

Misoprostol treatment decreases neuronal death but not bleeding volume in the collagenase-induced ICH model. (A) Fluoro-Jade B (FJB) histological staining in sections collected 3 days after collagenase injection revealed substantial degeneration of neurons and processes in the perihematomal region. Scale bar = 50 μm. Insets represent FJB-positive degenerating neurons at higher magnification. Compared with vehicle-treated mice, misoprostol-treated mice had 60% fewer FJB-positive neurons in the peri-ICH area on day 3 after ICH (n=8 mice/group, $^{**}p<0.01$, *t*-test). (B) Misoprostol treatment did not affect collagenase-induced bleeding. The level of hemoglobin content in the homogenate of injured striatum did not differ between misoprostol- and vehicle-treated mice when measured at 24 hours after ICH (n=6 mice/group, $p>0.05$). All values are means ± SD.

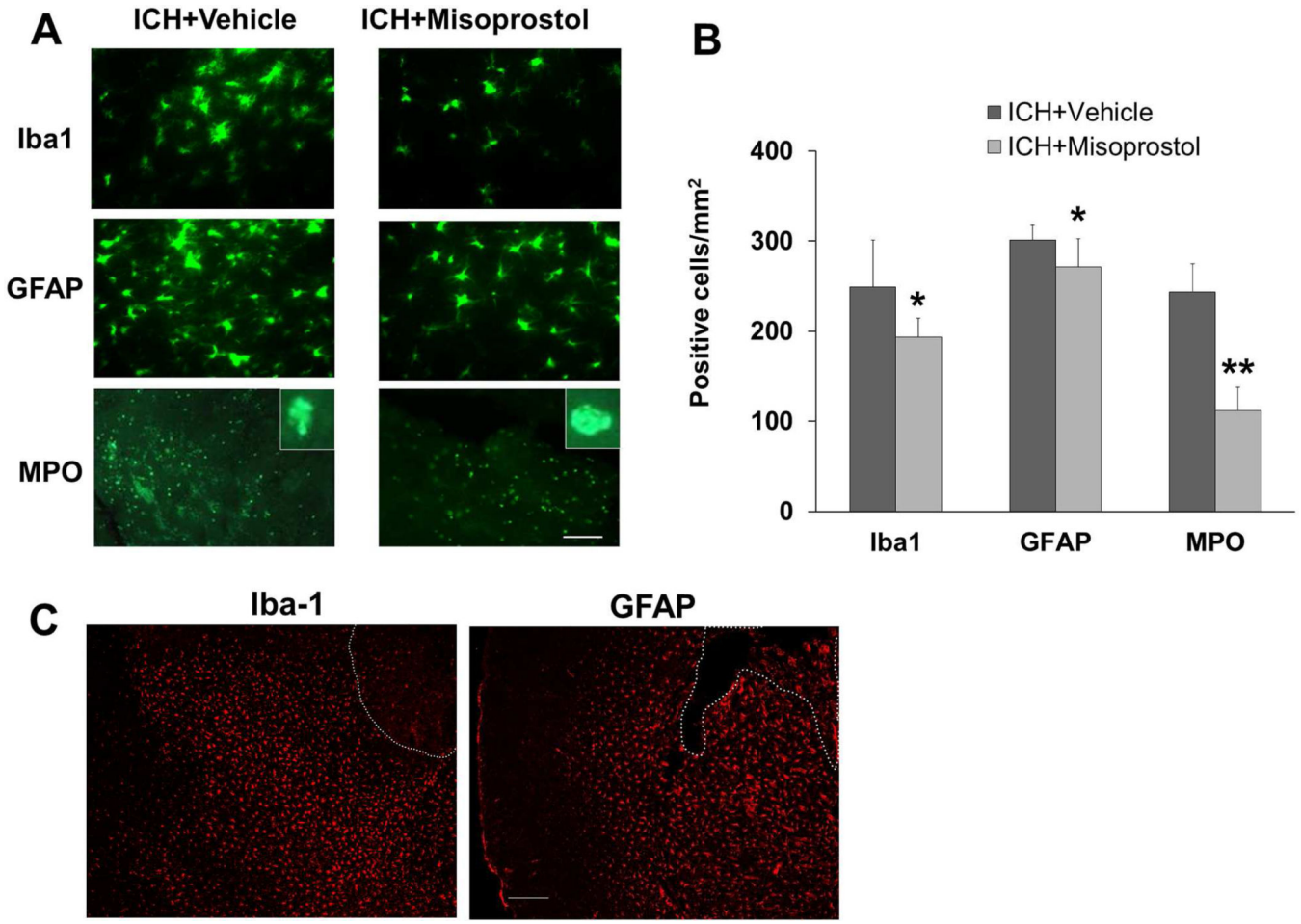

Fig. 4.

Misoprostol treatment decreases cellular inflammatory response in the collagenase-induced ICH model. (**A**) Activated microglia/macrophages (Iba1-immunoreactive cells), reactive astrocytes (GFAP-immunoreactive cells), and infiltrating neutrophils (MPO-immunoreactive cells) were evident around the injury site on day 3 after ICH. Insets represent MPO-positive cells at higher magnification. Scale bar = 40 μm. (**B**) Misoprostol treatment reduced the number of activated microglia/macrophages, activated astrocytes, and infiltrating neutrophils (n=8 mice/group, *p<0.05, **p<0.01, t-test). (**C**) Activated microglia/macrophages (amoeboid, Iba1-immunoreactive cells) and reactive astrocytes (GFAP-immunoreactive cells) were distributed equally around the hematoma on day 3 after collagenase-induced ICH. The dashed white lines indicate lesion edge. Scale bar = 50 μm. All values are means ± SD.

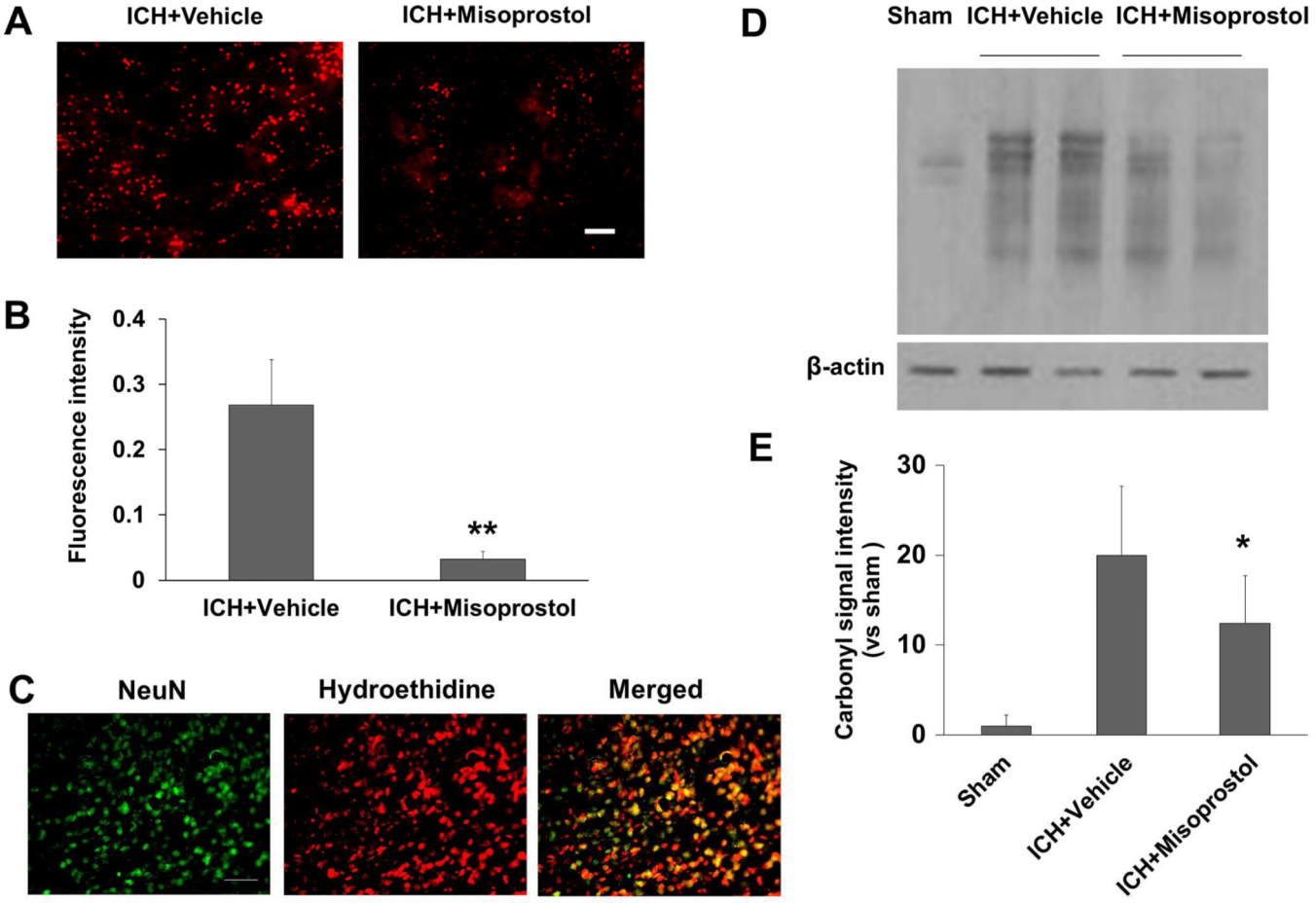

Fig. 5.

Misoprostol treatment decreases superoxide production and protein oxidation in the collagenase-induced ICH model. (**A**) Superoxide production was measured by dihydroethidium fluorescence, which was evident in the perihematomal region on day 1 after ICH in vehicle-treated mice (left). Misoprostol treatment attenuated dihydroethidium fluorescence intensity (right). Scale bar = 30 μm. (**B**) Bar graph shows quantification analysis of dihydroethidium fluorescence intensity in the perihematomal region on day 1 after ICH (n=5 mice/group, $^{**}p<0.01$, *t*-test). (**C**) Increased ethidium signals (small red particles) were detected mostly in NeuN-positive neuronal nucleus (green) in the perihematomal region on day 1 after ICH (n=5 mice). Scale bar = 40 μm. (**D**) OxyBlot analysis identified protein carbonyl groups in the damaged striatum on day 1 after ICH in vehicle-treated mice. Misoprostol treatment attenuated carbonyl formation. (**E**) Bar graph shows quantification analysis of carbonyl immunoreactivity on multiple protein bands in the hemorrhagic hemisphere on day 1 after ICH (n=5 mice/group, $^{*}p<0.05$, *t*-test). All values are means ± SD.

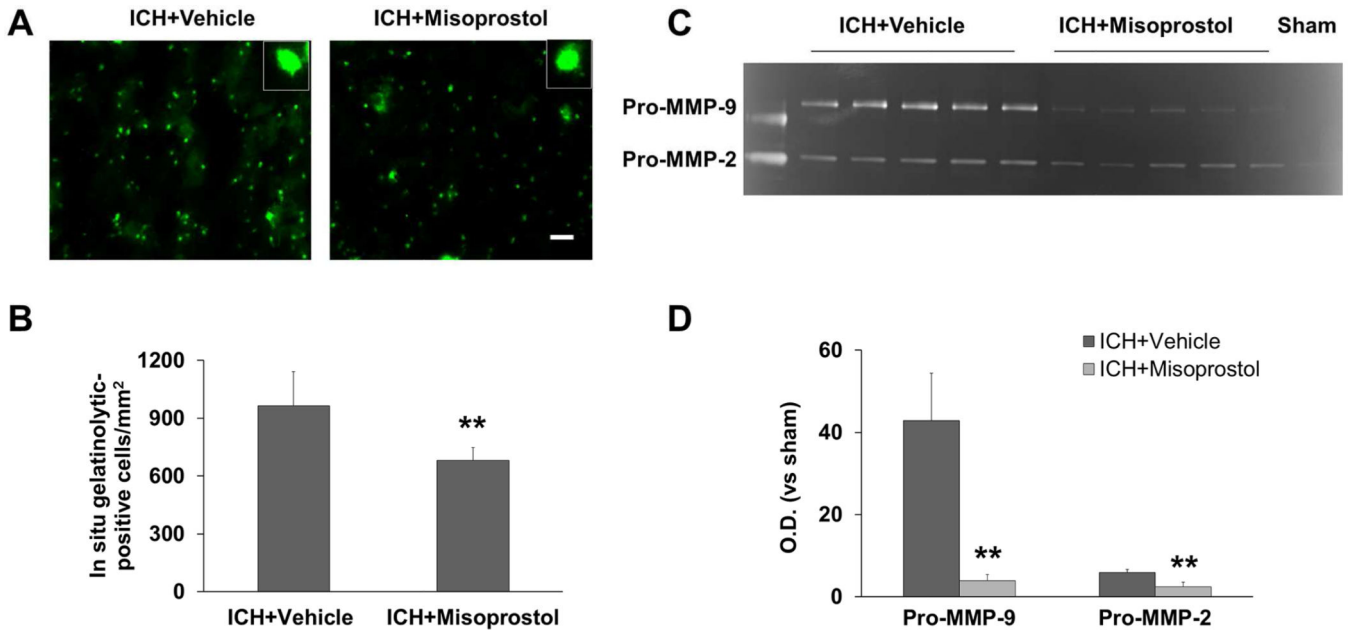

Fig. 6.

Misoprostol treatment decreases gelatinolytic activity in the collagenase-induced ICH model. (**A**) On day 1 after ICH, gelatinolytic activity measured by in situ gelatin zymography was increased in the perihematomal region in mice treated with vehicle (left). Gelatinolytic activity was reduced in mice treated with misoprostol (right). Insets represent gelatinolytic activity-positive cells at higher magnification. Scale bar = 30 μm. (**B**) Bar graph shows quantification analysis of gelatinolytic-positive cells in the perihematomal region on day 1 after ICH (n = 5 mice/group). (**C**) On day 1 after ICH, gelatin gel zymography revealed gelatinolytic activity, visible as white bands on gels where gelatin was degraded. Pro-MMP-9 bands (98 kDa) and pro-MMP-2 bands (72 kDa) are evident. Activity of both pro-MMP-9 and pro-MMP-2 was increased in the hemorrhagic hemisphere; misoprostol treatment attenuated the increase. (**D**) Bar graph shows quantification analysis of optical density (O.D.) of pro-MMP-9 and pro-MMP-2 activity on day 1 after ICH (n=5 mice/group). All values are means ± SD; $^{**}p<0.01$, *t*-test.

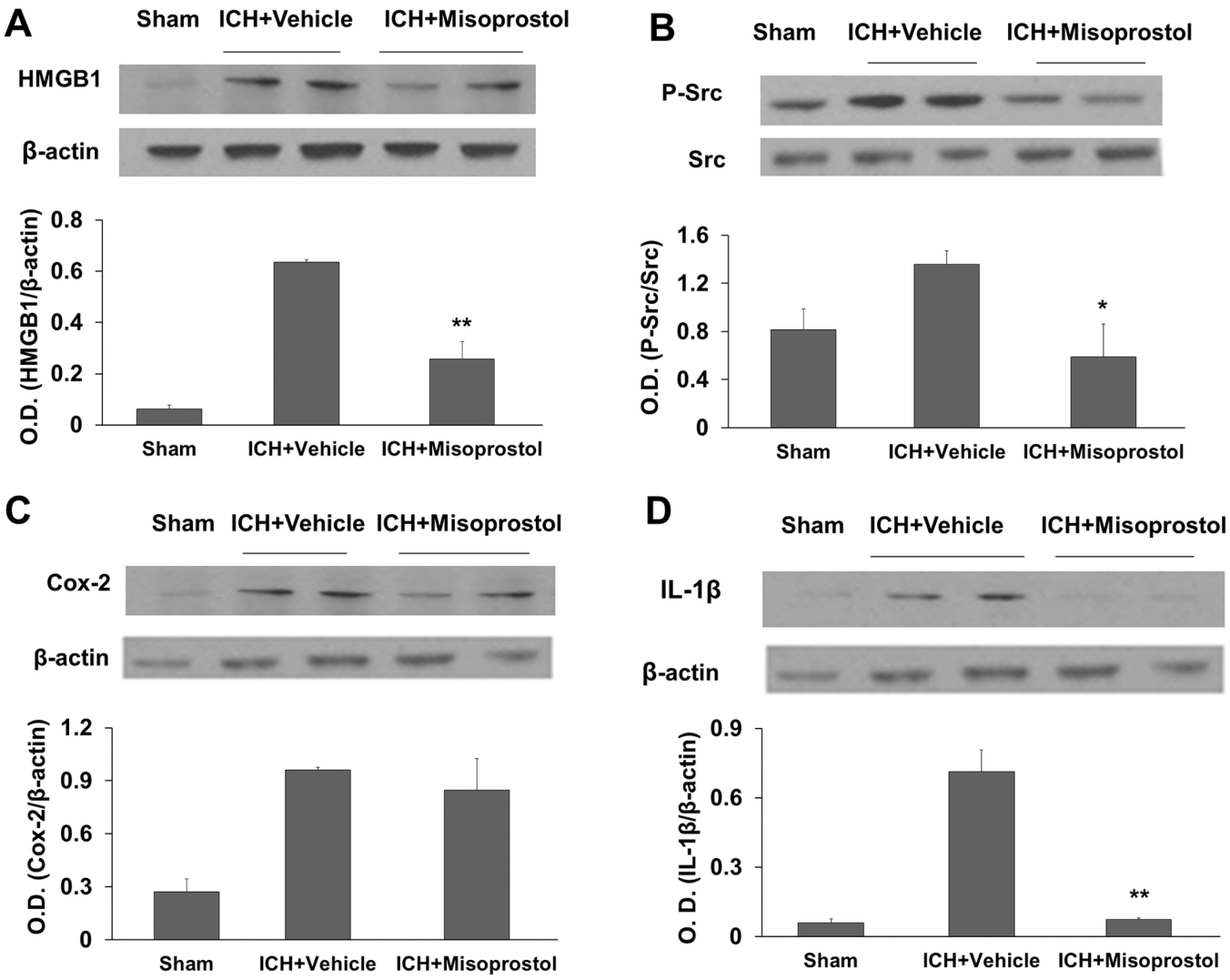

Fig. 7.

Misoprostol treatment decreases HMGB1 expression, Src kinase activity, and IL-1β expression in the collagenase-induced ICH model. (**A–D**) Western blot analysis shows the effects of misoprostol treatment on levels of HMGB1 (**A**), phosphorylated (P−) and total Src (**B**), COX-2 (**C**), and IL-1β (**D**) in the hemorrhagic hemisphere on day 1 after ICH. β-actin and total Src were used as loading controls. Misoprostol treatment reduced immunoreactivity of HMGB1, phosphorylated Src, and IL-1β, but not COX-2 on day 1 after ICH. O.D., optical density. n=5 mice/group; All values are means ± SD; **p*<0.05, ***p*<0.01, *t*-test.

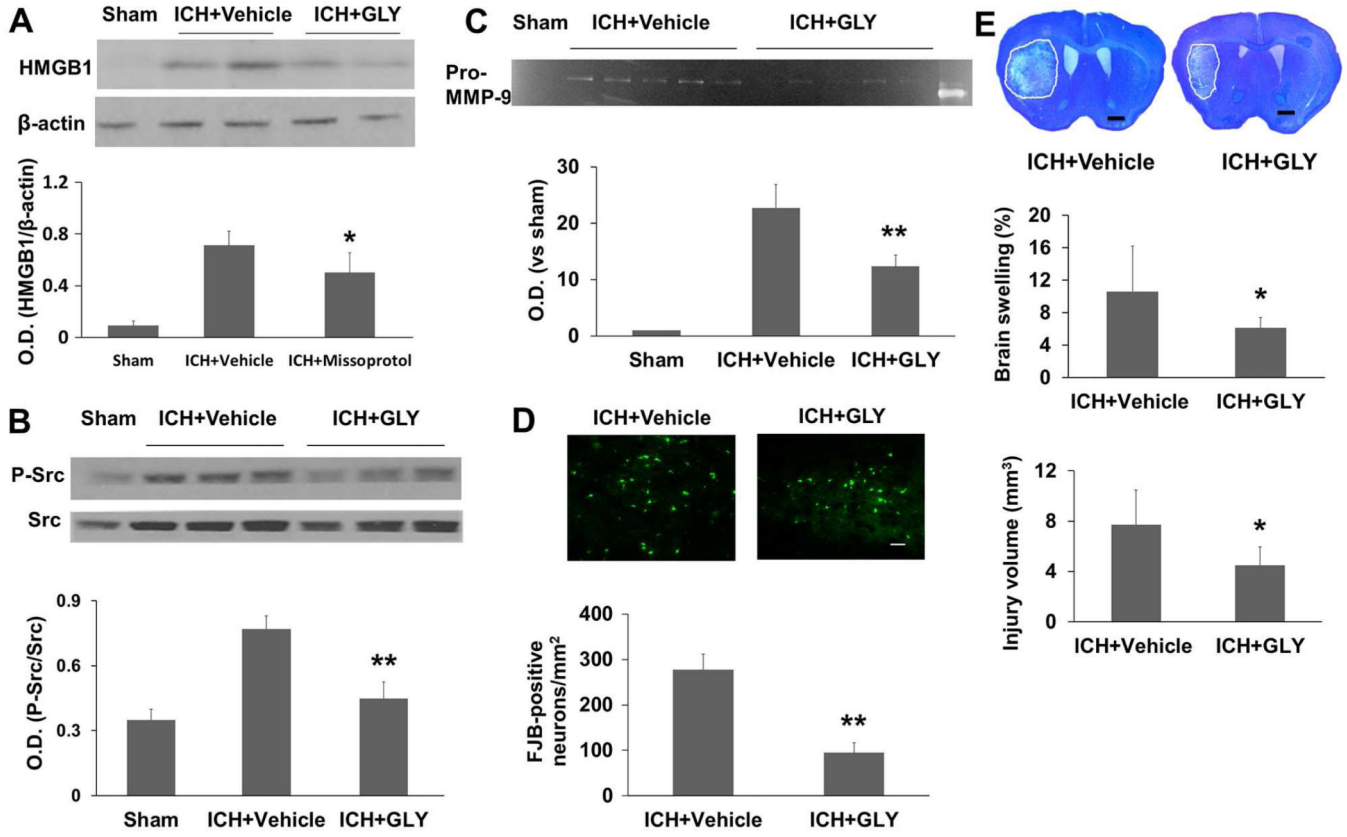

Fig. 8.

HMGB1 inhibition with glycyrrhizin (GLY) is protective in the collagenase-induced ICH model. Western blot analysis showed that glycyrrhizin treatment reduced immunoreactivity of HMGB1 (**A**) and phosphorylated (P−) Src (**B**) on day 1 after ICH (n=5 mice/group). (**C**) Gelatin gel zymography analysis showed that glycyrrhizin treatment reduced the activity of pro-MMP-9 on day 1 after ICH (n=5 mice/group). (**D**) Glycyrrhizin treatment reduced the number of Fluoro-Jade B (FJB)-positive cells in the perihematomal region on day 3 after ICH (n=8 mice/group). Scale bar = 30 μm. (**E**) Histologic staining with Luxol fast blue/Cresyl Violet showed that glycyrrhizin treatment decreased brain swelling by 42.5% and lesion volume by 41.8% on day 3 after ICH (n=8 mice/group). O.D., optical density. All values are means ± SD; *$p<0.05$, **$p<0.01$, *t*-test.

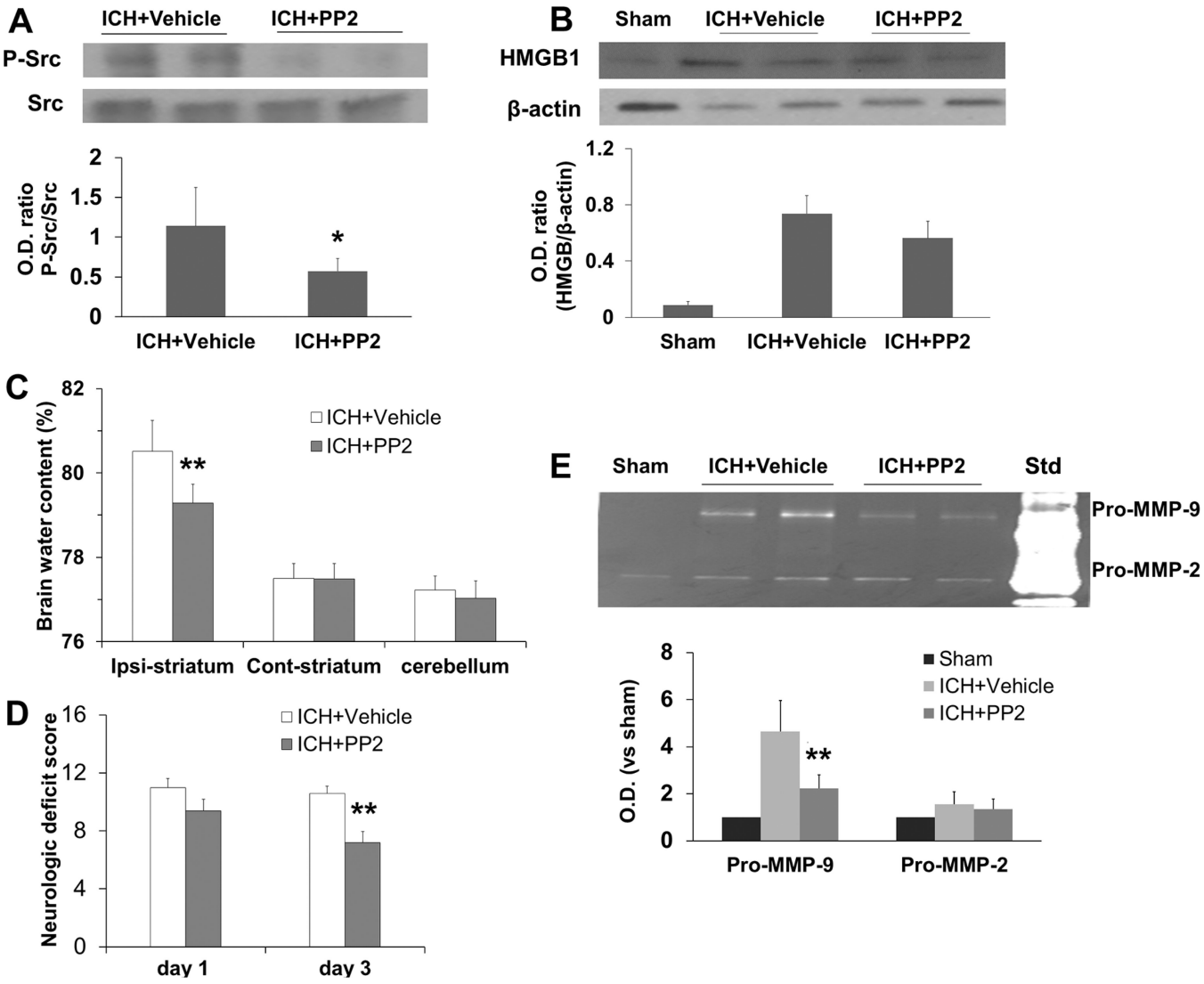

Fig. 9.

Src kinase inhibition with PP2 is protective in the collagenase-induced ICH model. (**A, B**) Western blot analysis showed that PP2 treatment reduced the level of phosphorylated (P−) Src, but not HMGB1 protein levels on day 1 after ICH (n=5 mice/group). Src kinase inhibition with PP2 decreased brain water content in the ipsilateral striatum (**C**) and neurologic deficit score (**D**) on day 3 after ICH (both n=6 mice/group). (**E**) Gelatin gel zymography showed that Src kinase inhibition with PP2 reduced the activity of pro-MMP-9 (98 kDa band), but not pro-MMP-2 (72 kDa band), on day 1 after ICH (n=5 mice/group). Std, mouse gelatinase standards. O.D., optical density; Ipsi, ipsilateral; Cont, contralateral. All values are means ± SD; *$p<0.05$, **$p<0.01$, *t*-test.